



HAL
open science

New insights into the accessibility of native cellulose to environmental contaminants toward tritium behavior prediction

A-L. Nivesse, N. Baglan, G. Montavon, O. Péron

► **To cite this version:**

A-L. Nivesse, N. Baglan, G. Montavon, O. Péron. New insights into the accessibility of native cellulose to environmental contaminants toward tritium behavior prediction. *J.Hazard.Mater.*, 2021, 420, pp.126619. 10.1016/j.jhazmat.2021.126619 . hal-03335498

HAL Id: hal-03335498

<https://hal.science/hal-03335498>

Submitted on 2 Aug 2023

HAL is a multi-disciplinary open access archive for the deposit and dissemination of scientific research documents, whether they are published or not. The documents may come from teaching and research institutions in France or abroad, or from public or private research centers.

L'archive ouverte pluridisciplinaire **HAL**, est destinée au dépôt et à la diffusion de documents scientifiques de niveau recherche, publiés ou non, émanant des établissements d'enseignement et de recherche français ou étrangers, des laboratoires publics ou privés.



Distributed under a Creative Commons Attribution - NonCommercial 4.0 International License

1 New insights into the accessibility of native cellulose to
2 environmental contaminants toward tritium behavior prediction

3

4 A-L. Nivesse^{1,2}, N. Baglan³, G. Montavon¹, O. Péron^{1*}

5

6 ¹SUBATECH, UMR 6457, 4, rue Alfred Kastler, BP 20722, 44307 Nantes Cedex 3, France

7 ²CEA, DAM, DIF, F-91297 Arpajon, France

8 ³CEA, DIF, DRF, JACOB, IRCM, SREIT, LRT, F-91297 Arpajon, France

9 *olivier.peron@subatech.in2p3.fr

10

11

12 **Highlights**

- 13 • Hydroxyl reactivity of native cellulose is correlated to its crystallinity.
- 14 • A linear relationship describes OH group accessibility versus Crystallinity Index.
- 15 • Fast XRD analysis gives access to hydroxyl reactivity of native cellulose.
- 16 • Tritium retention capacity of native cellulose is deduced from the model.
- 17 • The model is applicable to environmental samples depending on cellulose parameters.

18

19 **Abstract**

20 Tritium speciation and behavior in the environment directly rely on accessible OH groups of
21 organic molecules and their hydrogen exchangeability properties. As one of the most widespread
22 biomolecule, cellulose role in reducing the exchange capacity of the hydrogen atom has been
23 previously highlighted experimentally in various environmental matrices. In this paper, a robust
24 and reliable T/H gas-solid isotopic exchange procedure has been implemented to assess the OH
25 group accessibility of native celluloses with an increasing degree of crystallinity. A linear
26 relationship was found between hydroxyl reactivity and the CrI of native
27 celluloses, as determined by the analysis of their crystalline structure from XRD characterization.
28 The application of the obtained linear experimental model to cellulosic materials was then
29 evaluated and an acceptable minimum value of 12% for the CrI parameter on environmental
30 matrices could thus be established. The authors have therefore proposed an environmental
31 matrices relevant and efficient analytical process in order to determine the accessibility of native
32 cellulose hydroxyl groups to tritium in the environment from a single and quick sample
33 characterization procedure.

34

35

36 **Keywords:** tritium, speciation, isotopic exchange, cellulose, pollutants

37

38 **1. Introduction**

39 Tritium is the natural radioactive isotope of hydrogen and one of the main radionuclides released
40 into the environment by nuclear installations (IRSN, 2017). According to current forecasts, the
41 release rates of this radionuclide are expected to rise significantly over the upcoming decades from
42 changes in fuel management methods along with new tritium-emitting facilities, such as the
43 International Thermonuclear Experimental Reactor (ITER) and Evolutionary Power Reactor
44 (EPR) (ASN, 2010; Song et al., 2019). To understand the behavior of this radioactive pollutant in
45 the environment and thus evaluate its potential impact, the main scientific challenge calls for
46 identifying its mobility and bioavailability characteristics, which are mainly governed by its
47 speciation. In environmental matrices, tritium can integrate organic matter in the form of
48 organically bound tritium (OBT) by replacing stable hydrogen isotopes and taking up
49 exchangeable positions (exchangeable OBT) or else remaining in the molecule until its
50 degradation (non-exchangeable OBT) (Diabaté and Strack, 1993; Kim et al., 2013; Sepall and
51 Mason, 1961). As such, monitoring OBT has become a major concern in many countries for both
52 public and regulatory assurance and several studies have focused on the non-exchangeable form
53 (NE-OBT) as a reliable environmental marker (Kim et al., 2013; Péron et al., 2016; Baglan et al.,
54 2018; Nivesse et al., 2021a, 2021b). Among those previous investigations, cellulose has been
55 repeatedly identified as one of the organic molecule with great impact on OBT speciation and was
56 found to be responsible for the decrease in tritium exchangeability rates within various cellulosic
57 environmental matrices (Nivesse et al., 2021a; Péron et al., 2018). Beyond these properties
58 specific to the cellulose biomolecule, the work presented in Nivesse et al. (2021a) has also
59 highlighted the total control of major constituent over the hydrogen transfer mechanisms and OBT
60 speciation found in related environmental matrices. As the most abundant biopolymer on earth and
61 the main structural component of cell walls in plants, cellulose reactivity to hydrogen isotopes

62 binding is thus key to understanding tritium behavior in the environment and its transfer into food
63 chain samples.

64 In cellulose molecules, OBT speciation directly relies on accessible OH groups and their hydrogen
65 exchangeability properties. On the supramolecular level, cellulose is composed of linear chains of
66 D-glucose units linked together by (1→4)-beta-D-glycosidic bonds, subjected to aggregation into
67 microfibrils with a sheet organization and a two-phase morphology of crystalline and amorphous
68 regions. The crystalline structure of cellulose is highly ordered and originates from extensive
69 intra-molecular and intra-strand hydrogen bonding between OH groups. As a result, the
70 accessibility of cellulose hydroxyl groups undergoes a drastic reduction, as has been widely
71 demonstrated in the literature during crystalline structure investigations of various cellulose
72 compounds in hydrogen-deuterium exchange experiments (Lindh and Salmén, 2017; Reishofer
73 and Spirk, 2015). Nevertheless, no clear analytical relationship has ever been derived between
74 hydrogen exchangeability and degree of crystallinity in native cellulose. To a global extent,
75 several characterizations methods (SEM, TEM, FTIR, XRD, TGA ...) are usually combined to
76 assess the link between the crystalline morphology of cellulose and applications related to its OH
77 group's reactivity (Luzi et al., 2019; Melikoğlu et al., 2019; Trache et al., 2016). However,
78 simplified calculation method could also be fit for purpose in given conditions. For example, the
79 Crystallinity Index (CrI) determined after a single X-ray diffraction (XRD) analysis is commonly
80 used for quantifying the crystallinity rate of native cellulose (Hashem et al., 2020; Johar et al.,
81 2012; Luzi et al., 2019; Madivoli et al., 2016; Melikoğlu et al., 2019; Segal et al., 1959; Trache et
82 al., 2016). The present work therefore aims to provide a simple and environmental matrices
83 relevant linear model to describe OH group accessibility with respect to the Crystallinity Index
84 (CrI) from a series of five native celluloses. While CrI is determined by means of X-ray diffraction
85 (XRD), OH group accessibility is investigated by a robust and reliable T/H gas-solid isotopic
86 exchange procedure (Nivesse et al., 2021a, 2021b, 2020; Péron et al., 2018). By virtue of being

87 extracted or investigated from environmental sources, the application potential of the linear model
88 obtained for the cellulose accessibility determination can then be established for cellulosic
89 materials and from direct measurements conducted on environmental matrices.

90

91 **2. Materials and methods**

92 **2.1. Sample preparation and characterization**

93 Alpha (cellulose-C) and microcrystalline (cellulose-E) native celluloses extracted from cotton
94 sources (CAS number: 9004-34-6) were purchased from Sigma-Aldrich. The crystalline structures
95 of these celluloses were modified by partial destruction using ball-milling processes. A series of
96 five native celluloses with increasing crystalline ratios was produced from ball-milling with the
97 following parameters: cellulose-A (142 x g, 15 min) and B (84 x g, 10 min) from cellulose-C
98 (alpha cellulose); and cellulose-D (68 x g, 3 min) from cellulose-E (microcrystalline cellulose).
99 Cellulose-E refers to the microcrystalline cellulose previously studied in Péron et al., (2018).

100 An amorphous compound of silica SiO₂ (CAS number: 7631-86-9) was purchased from Sigma-
101 Aldrich and added in different ratios to each cellulose of the series (A through E) in order to
102 obtain a modified sequence of increasing cellulose content samples (from 5% to 95% by weight)
103 for each native cellulose of the series (Table 1).

104 All the samples were directly freeze-dried after the preparation steps and stored under vacuum
105 prior to further use.

106

107

108

109

110

111

112

113 **2.2. Experimental procedure**

114 *2.2.1. X-ray diffraction analysis*

115 X-ray diffraction was employed to determine the crystallinity of the series of five native celluloses
116 and the modified sequences of increasing cellulose content samples. Each milled powder material
117 was placed on the sample holder and leveled to obtain total and uniform X-ray exposure. Analyses
118 were performed at room temperature using a D5000 Bruker X-ray diffractometer (Cu/K α
119 radiation = 0.154 nm at 40 kV and 30 mA). The XRD patterns were collected within the range of
120 $2\theta = 0^\circ - 50^\circ$ with a scan step of $2\theta = 0.02^\circ$ and a measurement time per step of 4 s.

121 The Crystallinity Index (CrI) was determined based on the reflected intensity data, according to
122 the method developed by Segal et al., (1959), using the following Equation 1:

$$(\text{CrI}) (\%) = \frac{(I_{002} - I_{\text{am}})}{I_{002}} \times 100 \quad (1)$$

123

124 where I_{002} is the maximum diffracted intensity by the (002) plane at a 2θ angle of around 22° ,
125 while I_{am} is the minimum diffracted intensity at a 2θ angle of around 18° , representing the
126 intensity scattered by the amorphous region of the sample.

127

128

129 *2.2.2. Isotopic exchanges*

130 The (α_{iso}) parameter describes the isotopic exchangeable hydrogen pool versus total hydrogen
131 atoms in a specific matrix and is typically determined by a gas-solid isotopic exchange procedure.
132 The gas-solid isotopic exchange process has already been developed and described in previous
133 publications (Nivesse et al., 2021b; Péron et al., 2018); it is based on a sample set-up vapor phase

134 experiment performed in a confined glove box (Plas-Labs 890-THC) with controlled and stable
 135 temperature ($20.0^{\circ} \pm 0.1^{\circ}\text{C}$) and relative humidity ($85\% < \text{RH} < 88\%$) parameters. An isotopic
 136 steady state with a defined (T/H) ratio is established between a bath of KCl-saturated solution
 137 $\left(\left(\frac{T}{H}\right)_{l, bath}\right)$ with controlled tritium activities, a vapor phase confined in a glove box
 138 $\left(\left(\frac{T}{H}\right)_{g, vapor}\right)$, the water condensed at the sample surface $\left(\left(\frac{T}{H}\right)_{l, cond}\right)$ and the exchangeable
 139 organically bound tritium of the sample $\left(\left(\frac{T}{H}\right)_{s, E-OBT}\right)$, which can be described by Equation 2:

$$\left(\frac{T}{H}\right)_{l, bath} = \left(\frac{T}{H}\right)_{g, vapor} = \left(\frac{T}{H}\right)_{l, cond} = \left(\frac{T}{H}\right)_{s, E-OBT} \quad (2)$$

140

141 Isotopic exchanges were conducted on native celluloses following four tritium-enrichment
 142 experiments with tritium-rich baths ($\text{HTO} = 120, 300, 500$ and 700 Bq.L^{-1}). After 2 days of solid-
 143 gas contact time, the steady state was assumed to be reached, and solid samples were recovered at
 144 days 2, 3 and 4 to ensure the reproducibility and steady state of the system. Three baths aliquots
 145 were also collected at the steady state and kept at a temperature below 5°C prior to distillation.
 146 After liquid nitrogen immersion and freeze-drying, the solid samples were heat-treated in a tubular
 147 furnace (Eraly, France), where the organic matter was transformed into carbon dioxide and
 148 combustion water. Liquid samples (combustion waters and baths aliquots) were purified by
 149 distillation under atmospheric pressure after pH adjustment with sodium peroxide (Na_2O_2) as
 150 needed. The tritium activities were measured by means of liquid scintillation counting
 151 (PerkinElmer Wallac Quantulus 1220 model) using an Ultima Gold LLT cocktail. The detection
 152 limit was estimated at below 1 Bq.L^{-1} for a counting time of 24 hours and a blank value of 0.7
 153 counts per minute. A quench correction was applied for each measurement according to a
 154 quenching curve calculated after calibration with laboratory-prepared quenched standards.

155 At each steady state, a mean value of the combustion water from each matrix sample $\left(\frac{T}{H}\right)_{s, OBT}$
156 was obtained by averaging the measured sample values forming the plateau. A mean value of each
157 saline solution $\left(\frac{T}{H}\right)_{l, bath}$ was also obtained by averaging the three measured bath aliquot values.
158 The (α_{iso}) parameter could thus be determined as the slope of the plot of $\left(\frac{T}{H}\right)_{s, OBT}$ versus
159 $\left(\frac{T}{H}\right)_{l, bath}$, in accordance with the description provided in Equation 3:

$$\alpha_{iso} = \frac{\Delta\left(\frac{T}{H}\right)_{s, OBT}}{\Delta\left(\frac{T}{H}\right)_{l, bath}} \quad \text{Eq. 3}$$

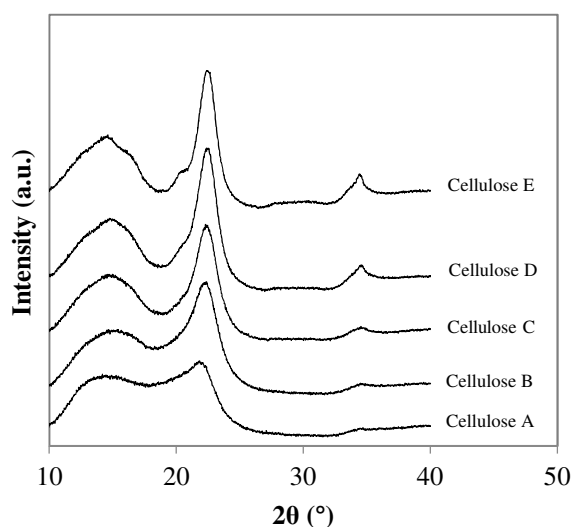
160

161

162 3. Results and discussion

163 3.1. Crystallinity Index (CrI) determination

164 The XRD patterns for the series of native celluloses are shown in Figure 1. All celluloses in the
165 series exhibited crystalline peaks attributed to the typical structure of cellulose I at: $2\theta = 16.1^\circ$
166 (110), 22° (200) and 34.7° (004) (Johar et al.,2012; Melikoğlu et al., 2019). Cellulose I is one of
167 the four allomorphic forms of crystalline cellulose (I to IV) and the most common form in a
168 natural source (Chen et al., 2011; Lu et al., 2013). CrI values for celluloses A, B, C, D and E were
169 calculated at 13, 34, 46, 55 and 62%, respectively. From celluloses E and C, the crystallinity ratio
170 decreases as expected due to the partial destruction of crystalline regions during the ball-milling
171 process (Sun and Cheng, 2002).



172
173 **Fig. 1:** XRD patterns for the series of five native celluloses from cellulose A through cellulose E

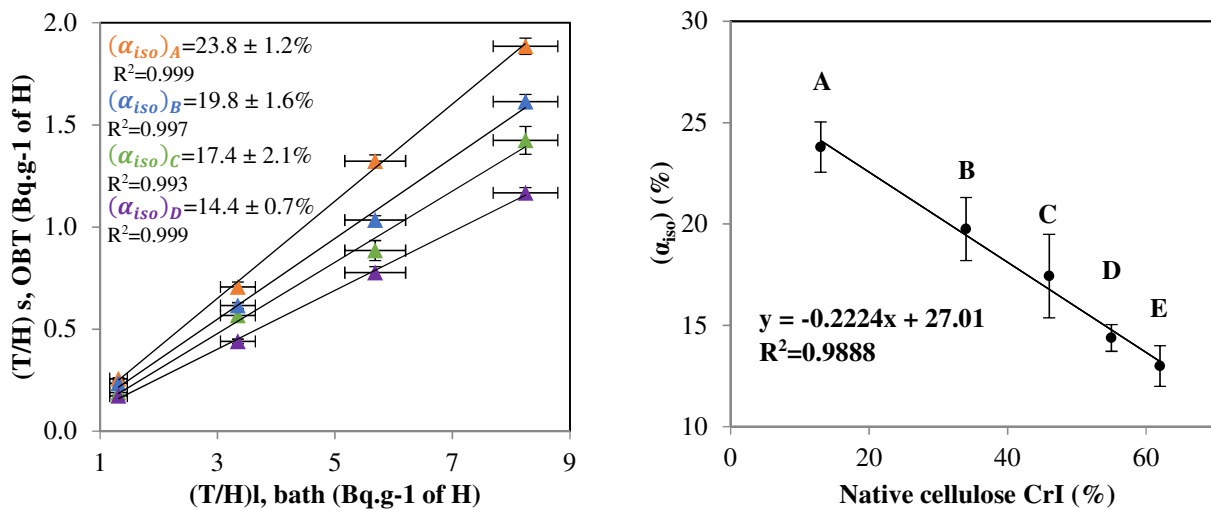
174
175 In order to assess the potential impact of the vapor phase contact during the gas-solid isotopic
176 exchange procedure onto the crystalline structure of the series of native celluloses, X-ray
177 diffraction analysis were conducted before and after the isotopic exchange step. Modifications on

178 both the intensity data of the XRD peaks (for the CrI calculation) and the allomorphic attribution
 179 (cellulose I allomorphic form) were thus established to be negligible as no significant change was
 180 observed on any of the samples.

181

182 3.2. Linear experimental model for the cellulose accessibility determination

183 Isotopic exchanges were conducted on native celluloses to assess their exchangeable parameter
 184 (α_{iso}). Accurate values of (α_{iso}) equal to $23.8 \pm 1.2\%$ ($R^2 = 0.999$), $19.8 \pm 1.6\%$ ($R^2 = 0.997$),
 185 $17.4 \pm 2.1\%$ ($R^2 = 0.993$), $14.4 \pm 0.7\%$ ($R^2 = 0.999$) and $13 \pm 1\%$ ($R^2 = 0.990$) were obtained for
 186 celluloses A through E, respectively (Fig. 2). The results on cellulose E exchangeable parameter
 187 (α_{iso}) were previously presented in Péron et al., (2018).



(a)

(b)

188 **Fig. 2:** (a) (T/H) of celluloses A through D in the steady state after freeze-drying vs. measured set
 189 (T/H) of saline solutions and their associated exchangeable parameter (α_{iso}). (b) Exchangeable
 190 parameter (α_{iso}) vs. Crystallinity Index (CrI) for the series of five native celluloses from A
 191 through E.

192

193 From these findings, an experimental model based on (α_{iso}) vs. CrI was obtained for the series of
194 native celluloses (Fig. 2). A decrease in the exchangeability parameter (α_{iso}) can be observed as
195 the degree of crystallinity in the cellulose molecule increases. The crystalline structure of cellulose
196 is represented by an orderly arrangement of D-glucose chains generated by hydrogen bonds. The
197 (1→4)-beta-D-glycosidic bonds and monomer arrangements oriented at 180° are thus responsible
198 for a three-dimensional network (see SI-1). Hence, hydroxyl groups of D-glucose units behave
199 like hydrogen-bound donors at both the intra-molecular and intra-strand levels to provide a
200 stabilized structure to cellulose (Jarvis, 2003; Nishiyama et al., 2003, 2002). As such, a larger
201 proportion of the hydrogen atoms is made inaccessible for isotopic exchange and behaves as non-
202 exchangeable hydrogen, while the degree of crystallinity in the cellulose is increasing.

203 The experimental model constructed with the series of native celluloses exhibits a linear tendency,
204 with a correlation coefficient equal to 0.9888. Hence, the suggestion of a proportionality ratio is
205 entirely noticeable between the decreases in hydrogen atom accessibility and the extent of the
206 crystalline phase in native cellulose. This dependency can therefore be described as linear
207 (Equation 4):

$$(\alpha_{iso_{celluloses}}) = -0.2224 \times (\text{CrI}) + 27.01 \quad \text{Eq. 4}$$

208

209 where ($\alpha_{iso_{celluloses}}$) is the exchangeable hydrogen atom ratio of the native celluloses series, in %,
210 and (CrI) the crystallinity index from 13 to 62 %.

211 Equation 4 can thus serve to deduce the ratio of exchangeable hydrogen atoms in native cellulose
212 molecules merely from information on the degree of crystallinity. Hence, these findings could
213 give access to the tritium under the form of NE-OBT storage capacities of native cellulose
214 molecules from a single XRD analysis.

215

3.3. Environmental matrices applications and limits

216
217 Investigations on organically bound tritium distribution and speciation towards cellulose pertain to
218 environmental cellulosic organic matter (Nivesse et al., 2021a; Péron et al., 2018). Consequently,
219 the linear model method established to determine cellulose accessibility requires applicability to
220 cellulosic materials from direct environmental matrices CrI measurements. In environmental
221 matrices, native cellulose may display a wide range of crystallinity rates and is always found in
222 combination with other amorphous to semi-amorphous compounds. An XRD analysis on the
223 entire environmental sample might therefore detect the attributed peak at 22° for the cellulose
224 needed for a CrI calculation, yet with a significant impact lowering its intensity in proportion with
225 the amorphous compound content. At some point, the presence of this amorphous phase, provided
226 by the other constituents, may become too great compared to the crystalline phase of the cellulose,
227 making the cellulose peak at 22° undetectable by means of XRD analysis. Nevertheless, it is
228 important to recall here that the main point of this study was to provide reliable information on the
229 accessibility of cellulose OH group from a very simplified and unique sample characterization, as
230 XRD measurements. In order to assess the applicability of the linear experimental model to
231 cellulosic materials from direct measurements in environmental matrices, a study of the significant
232 limits of the CrI parameter determination from XRD analysis was thus carried out. For this
233 purpose, each native cellulose of the series was mixed in different ratios with SiO_2 amorphous
234 compounds to simulate other non-crystalline fractions of environmental matrices and then
235 analyzed by XRD. CrI (%) values for the modified sequences of increasing cellulose content
236 samples are presented in Table 1. From these results and the cellulose content (in % by weight) of
237 each sample, theoretical CrI values could be calculated and attributed to each of the studied native
238 celluloses (calculated native cellulose CrI (%)) and compared to their actual CrI values (actual
239 native cellulose CrI (%)) (Table 1). For each modified sequence, the cellulose contents were

240 adapted in each sample to achieve the minimum content of cellulose needed to reach the actual
 241 calculated CrI value.

242

243

244

245

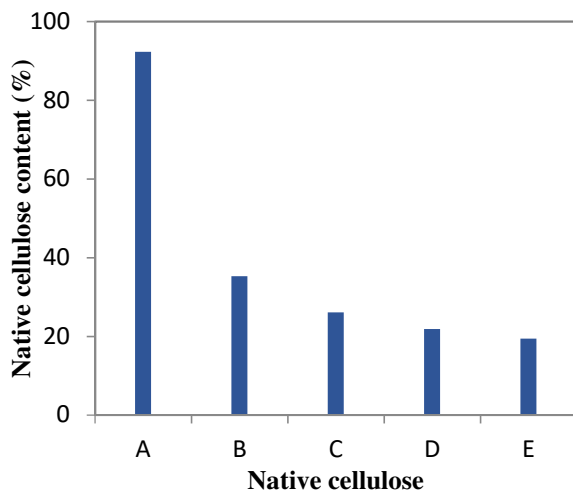
Native cellulose sequence	Sample	Native cellulose ratio (in % by weight)	Sample CrI (%)	Calculated native cellulose CrI (%)	Actual native cellulose CrI (%)
Cellulose A	A-1	60,3	-	-	13
	A-2	70,2	-	-	
	A-3	80,0	4	5	
	A-4	90,4	8	10	
	A-5	94,8	12	13	
Cellulose B	B-1	20,2	4	18	34
	B-2	30,0	9	30	
	B-3	35,6	12	34	
	B-4	40,1	14	34	
	B-5	50,1	17	34	
Cellulose C	C-1	15,5	4	26	46
	C-2	20,3	8	40	
	C-3	26,1	12	46	
	C-4	30,3	14	46	
	C-5	40,1	18	46	
Cellulose D	D-1	15,0	8	50	55
	D-2	19,6	11	54	
	D-3	23,2	13	55	
	D-4	30,3	17	55	
	D-5	40,3	22	55	
Cellulose E	E-1	10,2	6	56	62
	E-2	14,5	9	60	
	E-3	20,4	13	62	
	E-4	25,3	16	62	
	E-5	30,1	19	62	

246

247 **Table 1:** Results on modified sequences of increasing cellulose content samples from celluloses A
 248 through E, along with their respective native cellulose ratio (% by weight), obtained sample CrI
 249 (%), and the resulting calculated native cellulose CrI (%) compared to the actual native cellulose
 250 CrI (%).

251

252 Results obtained on the minimum content in % by weight of native celluloses A through E needed
253 to effectively reach an XRD analysis peak at 22° for the correct calculation of their respective CrI
254 values are presented in Figure 3. For medium to highly crystalline cellulose (i.e. celluloses B
255 through E), the minimum cellulose content needed in samples was found to lie around 20% to
256 35% by weight. These values are by far lower than the minimum content of cellulose in natural
257 cellulosic sources like trees or cotton, yet which does approximately correspond to that found in
258 green cellulosic plants like grass or tree leaves (Sun and Cheng, 2002). For very weak crystalline
259 cellulose (cellulose A), only a very high cellulose content was found to be acceptable for an
260 accurate cellulose CrI determination from XRD analysis.



261

262 **Fig. 3:** Minimum content (% by weight) of native celluloses A through E needed to effectively
263 reach an XRD analysis peak at 22° for the accurate calculation of their respective CrI (%)

264

265 For each of the native cellulose results, it was then estimated that the minimum CrI value
266 calculated from XRD analysis was acceptable as of 12% in an environmental sample to produce
267 an accurate cellulose CrI deduction. Nevertheless, this value remains dependent on the typical
268 internal parameters used in a cellulose analysis of the XRD equipment and could thus be further

269 improved, as needed. Similarly, this information proves to be relevant when cellulose is the only
270 constituent of the studied matrix whose crystallinity is directly related to the XRD analysis peak at
271 22°. The linear model is therefore applicable to environmental matrices for cellulose accessibility
272 determination under this condition whenever the CrI value obtained from the matrix sample XRD
273 analysis exceeds 12%. A complementary analysis of the sample composition in cellulose is then
274 needed to deduce the CrI and, hence, the accessibility of the studied cellulose to the main
275 radionuclide released by nuclear power plants, tritium. A fast and efficient analytical process is
276 therefore available for further investigations on organic tritium retention capacities of cellulosic
277 environmental matrices and should also be of great interest to understanding tritium behavior into
278 other major constituents in food chain samples like proteins.

279 Besides radioactive pollution concerns, the exchange capacities of OH group hydrogen atoms in
280 native cellulose are also important in other hydrogen isotope-related topics, such as investigations
281 on cellulosic material origins within protium and deuterium ratios, to the same extent as in the
282 field of nuclear forensics and retrospective studies on tritium releases into the environment. Most
283 of the functional properties of the cellulose polymer derives from its hydroxyl groups since its
284 chemical reactivity is mainly a function of the high donor reactivity of its OH groups (Klemm et
285 al., 2005; O'Connell et al., 2008). The hydrogen exchange properties of these OH groups are then
286 heavily involved in the binding processes of metal ions into cellulose fibers, from sorption
287 supported by a hydrated shell exchange with OH groups or electrostatic interactions with carboxyl
288 groups (Kongdee and Bechtold, 2009; Öztürk et al., 2009). As such, the established linear model
289 could also find an interest to estimate the complexing capacities of cellulose with transition metals
290 and actinides in its natural state in environmental samples.

291

292

293

294 **4. Conclusion**

295 To improve the scientific knowledge on tritium behavior prediction in the environment, hydroxyl
296 reactivity has been investigated in a series of native celluloses with an increasing degree of
297 crystallinity using a robust and reliable T/H gas-solid isotopic exchange procedure. A linear
298 relationship was derived between OH group accessibility to tritium and the Crystallinity Index
299 (CrI) of native celluloses. Since the purpose of this study relies on natural cellulose sources, the
300 applicability of the linear model from direct measurements on environmental matrices was
301 investigated with samples of increasing cellulose content at various crystallinity rates. An
302 acceptable minimum value of 12% for the CrI parameter on environmental matrices could thus be
303 established for the direct deduction of an accurate cellulose content CrI and OH accessibility.
304 These findings then make it possible to determine efficiently, by means of a single and fast XRD
305 analysis, the accessibility of the entire cellulose hydroxyl group pool to tritium bound into
306 environmental matrices. This information can subsequently be used not only to highlight the
307 hydrogen isotopes including tritium storage capacities in cellulosic environmental matrices, but
308 also to evaluate the contribution of other complex compounds involved with structures difficult to
309 characterize, like proteins. Applications to investigations on cellulosic material origins could
310 emerge, to the same extent as retrospective studies of tritium releases and nuclear forensics. In a
311 more fundamental manner, this method of determining hydroxyl group accessibility on native
312 cellulose also provides much relevance in understanding the involvement of the polymer in
313 environmental matrices accessibility to deuterium and tritium, as well as in grasping complexing
314 capacities with metals in the environment.

315

316 **References**

- 317 ASN, (2010). Le livre blanc du tritium, groupes de réflexion menés de mai 2008 à avril 2010 sous
318 l'égide de l'ASN.
- 319 Baglan, N., Cossonnet, C., Roche, E., Kim, S. B., Croudace, I., & Warwick, P. (2018). Feedback
320 of the third interlaboratory exercise organised on wheat in the framework of the OBT
321 working group. *Journal of environmental radioactivity*, 181, 52-61.
- 322 Chen, W., Yu, H., Liu, Y., Chen, P., Zhang, M., Hai, Y., (2011). Individualization of cellulose
323 nanofibers from wood using high-intensity ultrasonication combined with chemical
324 pretreatments. *Carbohydrate Polymers* Vol. 83(4), 1804–1811.
- 325 Diabaté, S., Strack, S., (1993). Organically bound tritium. *Health Physics* Vol. 65(6), 698–712.
- 326 Hashem, M.A., Elnagar, M.M., Kenawy, I.M., Ismail, M.A., (2020). Synthesis and application of
327 hydrazono-imidazoline modified cellulose for selective preparation of precious metals
328 from geological samples. *Carbohydrate Polymers* Vol. 237.
- 329 IRSN, (2017). Rapport Actualisation des connaissances Tritium Environnement. Editor : Institut
330 de Radioprotection et de Sûreté Nucléaire (IRSN).
- 331 Jarvis, M., (2003). Chemistry: cellulose stacks up. *Nature* Vol. 426, 611–612.
- 332 Johar, N., Ahmad, I., Dufresne, A., (2012). Extraction, preparation and characterization of
333 cellulose fibres and nanocrystals from rice husk. *Industrial Crops and Products* Vol. 37(1),
334 93–99.
- 335 Kim, S.B., Baglan, N., Davis, P.A., (2013). Current understanding of organically bound tritium
336 (OBT) in the environment. *Journal of Environmental Radioactivity* Vol. 126(1), 83–91.
- 337 Klemm, D., Heublein, B., Fink, H.-P., Bohn, A., (2005). Cellulose: Fascinating Biopolymer and
338 Sustainable Raw Material. *Angewandte Chemie International Edition* Vol. 44(22), 3358–
339 3393.
- 340 Kongdee, A., Bechtold, T., (2009). Influence of ligand type and solution pH on heavy metal ion
341 complexation in cellulosic fibre: model calculations and experimental results. *Cellulose*
342 Vol. 16(1), 53–63.
- 343 Lindh, E.L., Salmén, L., (2017). Surface accessibility of cellulose fibrils studied by hydrogen-
344 deuterium exchange with water. *Cellulose* Vol. 24(1), 21–33.
- 345 Lu, H., Gui, Y., Zheng, L., Liu, X., (2013). Morphological, crystalline, thermal and
346 physicochemical properties of cellulose nanocrystals obtained from sweet potato residue.
347 *Food Research International* Vol. 50(1), 121–128.
- 348 Luzi, F., Puglia, D., Sarasini, F., Tirillò, J., Maffei, G., Zuurro, A., Lavecchia, R., Kenny, J.M.,
349 Torre, L., (2019). Valorization and extraction of cellulose nanocrystals from North African
350 grass: *Ampelodesmos mauritanicus* manuscript. *Carbohydrate Polymers* 209, 328–337.

- 351 Madivoli, E., Kareru, P., Gachanja, A., Mugo, S., Murigi, M., Kairigo, P., Kipyegon, C.,
352 Mutembei, J., Njonge, F., (2016). Adsorption of Selected Heavy Metals on Modified Nano
353 Cellulose. *International Research Journal of Pure and Applied Chemistry* Vol. 12, 1–9.
- 354 Melikoğlu, A.Y., Bilek, S.E., Cesur, S., (2019). Optimum alkaline treatment parameters for the
355 extraction of cellulose and production of cellulose nanocrystals from apple pomace.
356 *Carbohydrate Polymers* Vol. 215(1), 330–337.
- 357 Nishiyama, Y., Langan, P., Chanzy, H., (2002). Crystal structure and hydrogen-bonding system in
358 cellulose II-beta from synchrotron X-ray and neutron fiber diffraction. *J. Am. Chem. Soc.*
359 Vol. 124, 9074–9082.
- 360 Nishiyama, Y., Sugiyama, J., Chanzy, H., Langan, P., (2003). Crystal structure and hydrogen
361 bonding system in cellulose II-alpha from synchrotron X-ray and neutron fiber diffraction.
362 *Am. Chem. Soc.* Vol. 125, 14300–14306.
- 363 Nivresse, A.-L., Baglan, N., Montavon, G., Granger, G., Péron, O., (2021a). Cellulose, proteins,
364 starch and simple carbohydrates molecules control the hydrogen exchange capacity of bio-
365 indicators and foodstuffs. *Chemosphere*.
- 366 Nivresse, A.-L., Baglan, N., Montavon, G., Granger, G., Péron, O., (2021b). Non-intrusive and
367 reliable speciation of organically bound tritium in environmental matrices. *Talanta*.
- 368 Nivresse, A.-L., Thibault de Chanvalon, A., Baglan, N., Montavon, G., Granger, G., Péron, O.,
369 (2020). An overlooked pool of hydrogen stored in humic matter revealed by isotopic
370 exchange: implication for radioactive ³H contamination. *Environmental Chemistry Letters*
371 Vol. 18(2), 475–481.
- 372 O’Connell, D.W., Birkinshaw, C., O’Dwyer, T.F., (2008). Heavy metal adsorbents prepared from
373 the modification of cellulose: A review. *Bioresource Technology* Vol. 99(15), 6709–6724.
- 374 Öztürk, H.B., Vu-Manh, H., Bechtold, T., (2009). Interaction of cellulose with alkali metal ions
375 and complexed heavy metals. *Lenzinger Berichte* 142–150.
- 376 Péron, O., Fourré, E., Pastor, L., Gégout, C., Reeves, B., Lethi, H.H., Rousseau, G., Baglan, N.,
377 Landesman, C., Siclet, F., Montavon, G., (2018). Towards speciation of organically bound
378 tritium and deuterium: Quantification of non-exchangeable forms in carbohydrate
379 molecules. *Chemosphere* Vol. 196(1), 120–128.
- 380 Péron, O., Gégout, C., Reeves, B., Rousseau, G., Montavon, G., & Landesman, C. (2016).
381 Anthropogenic tritium in the Loire River estuary, France. *Journal of Sea Research*, 118,
382 69-76.
- 383 Reishofer, D., Spirk, S., (2015). Deuterium and Cellulose: A Comprehensive Review. *Cellulose*
384 *Chemistry and Properties: Fibers, Nanocelluloses and Advanced Materials* Vol. 271, 93–
385 114.
- 386 Segal, L., Creely, J.J., Martin, A.E., Conrad, C.M., (1959). An Empirical Method for Estimating
387 the Degree of Crystallinity of Native Cellulose Using the X-Ray Diffractometer. *Textile*
388 *Research Journal* Vol. 29(10), 786–794.

- 389 Sepall, O., Mason, S.G., (1961). Hydrogen exchange between cellulose and water: II.
390 Interconversion of accessible and inaccessible regions. Canadian Journal of Chemistry
391 Vol. 39(10), 1944–1955.
- 392 Song, J., Xiong, Y., Lang, L., Shi, Y., Ba, J., Jing, W., & He, M. (2019). Radiochemical reaction
393 of DT/T2 and CO under high pressure. Journal of hazardous materials, Vol. 378, 120720.
- 394 Sun, Y., Cheng, J., (2002). Hydrolysis of lignocellulosic materials for ethanol production: a
395 review. Bioresource Technology Vol. 83, 1–11.
- 396 Trache, D., Hussin, M.H., Hui Chuin, C.T., Sabar, S., Fazita, M.R.N., Taiwo, O.F.A., Hassan,
397 T.M., Haafiz, M.K.M., (2016). Microcrystalline cellulose: Isolation, characterization and
398 bio-composites application—A review. International Journal of Biological
399 Macromolecules Vol. 93(1), 789–804.

400

401